Author Manuscript

Author Manuscript

Author Manuscript

Author Manuscript

HHS Public Access

Author manuscript

Exp Eye Res. Author manuscript; available in PMC 2020 November 18.

Published in final edited form as:

Exp Eye Res. 2020 April ; 193: 107957. doi:10.1016/j.exer.2020.107957.

Systemic hypoxia led to little retinal neuronal loss and dramatic optic nerve glial response

Louise Alessandra Mesentier-Louro[a], **Mohammed Ali Shariati**[a], **Roopa Dalal**[a], **Alexandra Camargo**[a], **Varun Kumar**[a], **Elya Ali Shamskhou**[c], **Vinicio de Jesus Perez**[c], **Yaping Joyce Liao**[a,b,*]

[a]Department of Ophthalmology, Stanford University, School of Medicine, Stanford, CA, USA

[b]Department of Neurology, Stanford University, School of Medicine, Stanford, CA, USA

[c]Department of Pulmonary Medicine, Stanford University, School of Medicine, Stanford, CA, USA

Abstract

Vision loss is a devastating consequence of systemic hypoxia, but the cellular mechanisms are unclear. We investigated the impact of acute hypoxia in the retina and optic nerve. We induced systemic hypoxia (10% O_2) in 6-8w mice for 48 h and performed in vivo imaging using optical coherence tomography (OCT) at baseline and after 48 h to analyze structural changes in the retina and optic nerve. We analyzed glial cellular and molecular changes by histology and immunofluorescence and the impact of pretreatment with 4-phenylbutyric acid (4-PBA) in oligodendroglia survival. After 48 h hypoxia, we found no change in ganglion cell complex thickness and no loss of retinal ganglion cells. Despite this, there was significantly increased expression of CCAAT-enhancer-binding protein homologous protein (CHOP), a marker of endoplasmic reticulum stress, in the retina and optic nerve. In addition, hypoxia induced obvious increase of GFAP expression in the anterior optic nerve, where it colocalized with CHOP, and significant loss of $Olig2^+$ oligodendrocytes. Pretreatment with 4-PBA, which has been shown to reduce endoplasmic reticulum stress, rescued total $Olig2^+$ oligodendrocytes and increased the pool of mature ($CC\text{-}1^+$) but not of immature (PDGFRa+) oligodendrocytes. Consistent with a selective vulnerability of the retina and optic nerve in hypoxia, the most striking changes in the 48 h murine model of hypoxia were in glial cells in the optic nerve, including increased CHOP expression in the astrocytes and loss of oligodendrocytes. Our data support a model where glial dysfunction is among the earliest events in systemic hypoxia – suggesting that glia may be a novel target in treatment of hypoxia.

Keywords

Hypoxia; Endoplasmic reticulum; ER stress; CHOP; Glia; Oligodendrocytes; Astrocytes; Retinal ganglion cells; Optic neuropathy

*Corresponding author. Department of Ophthalmology Stanford University Medical Center, 2452 Watson Court, Palo Alto, CA, 94303-5353. yjliao@stanford.edu (Y.J. Liao).

Appendix A. Supplementary data

Supplementary data to this article can be found online at https://doi.org/10.1016/j.exer.2020.107957.

Author Manuscript Author Manuscript Author Manuscript Author Manuscript

1. Introduction

The brain (Jha and Morrison, 2018) and retina (Caprara and Grimm, 2012) consume high levels of oxygen, so they are particularly vulnerable in systemic hypoxia. Systemic hypoxia can be caused by chronic lung disease or congenital heart disease and after ascent to high altitudes for sport or family vacation (Arjamaa and Nikinmaa, 2006). Visual disturbances and vision loss are well described at high altitudes and other conditions of systemic hypoxia (Linsenmeier and Zhang, 2017). While the retina is arguably more resistant to ischemia than the brain because of its dual blood supply (Wangsa-Wirawan and Linsenmeier, 2003), it is more susceptible to hypoxia than most of the central nervous system (CNS) because of its high energy demand. Indeed, retinal hypoxia has been described in the setting of retinopathy of prematurity (Hartnett and Penn, 2012), proliferative diabetic retinopathy (Guduru et al., 2016) and glaucoma (Tezel and Wax, 2004). Changes in retinal thickness and function measured by optical coherence tomography (OCT) and electroretinography were described following short-term exposure to high-altitude (Tian et al., 2018). Although vision changes following short-term exposure to hypoxia are typically reversible, some individuals may develop optic disc edema, subsequent optic atrophy, and irreversible vision loss due to exposure to high altitudes (Bandyopadhyay et al., 2002; Bosch et al., 2012; Schatz et al., 2018).

Hypoxia leads to many changes in the retinal neurons, and is the cause of blinding diseases like retinopathy of prematurity and proliferative diabetic retinopathy (Wangsa-Wirawan and Linsenmeier, 2003). The effect of hypoxia on retinal ganglion cells (RGCs) and their axons, which form the optic nerve, is particularly debilitating because they form the only connection to the brain for interpretation of visual information. A study of pattern electroretinography changes after 5-min inhalation of hypoxic gas in healthy adults demonstrated that RGCs are very sensitive to hypoxia (Kergoat et al., 2006). Severe hypoxia or ischemia leads to RGC death via apoptosis or necrosis (Kaur et al., 2008).

In addition to neurons, CNS hypoxia also affects glia. The CNS white matter tracts such as the corpus callosum and optic nerve are particularly susceptible to hypoxic injury (Ferriero, 2004), and damage to oligodendrocytes is a major cause of neurological impairment as a result of perinatal hypoxia in infants (Wang et al., 2018) and stroke in adults (Matute et al., 2013). For instance, brief focal ischemia causes oligodendrocytes to die as early as 3 h after arterial occlusion (Matute et al., 2013).

Following ischemic injury to the optic nerve and retina, we and others have shown activation of the unfolded protein response (UPR) pathway, with increased expression of the proapoptotic transcriptional regulator CCAAT-enhancer-binding protein homologous protein (CHOP) in animal models of nonarteritic anterior ischemic optic neuropathy (NAION) (Kumar et al., 2019), glaucoma (Doh et al., 2010; Hu et al., 2012), optic neuritis (Huang et al., 2017), diabetic retinopathy (Drel et al., 2009; Li et al., 2009; Oshitari et al., 2010, 2011), and N-methyl-D-aspartate (NMDA)-induced RGC loss (Shimazawa et al., 2012). Activation of the UPR can potentiate the effects of hypoxia-inducible factor family of transcriptional activators (Pereira et al., 2014). In mouse (Qi et al., 2004) and rat (Srinivasan and Sharma, 2011) studies of stroke, there was post-ischemic increase in CHOP, activation of caspase-12,

Author Manuscript Author Manuscript Author Manuscript Author Manuscript

and greater number of terminal deoxynucleotidyl transferase-mediated dUTP nick end labeling (TUNEL)-positive cells, indicating activation of endoplasmic reticulum (ER) stress and apoptotic pathways.

In this study, we investigated the impact of 48 h of systemic hypoxia on the retina and optic nerve. In addition, we investigated the therapeutic effects of the chemical chaperone 4-phenylbutyric acid (4-PBA) in reducing hypoxic damage.

2. Methods

2.1. Animals

All animal care and experiments were carried out in accordance with the Association for Research in Vision and Ophthalmology statement for the Use of Animals in Ophthalmic and Vision Research and with approval from the Stanford University Administrative Panel on Laboratory Animal Care. Adult wild-type C57BL/6 female mice (Charles River Laboratories, Inc., Hollister, CA, USA) were housed in cages at constant temperature, with a 12:12-h light/dark cycle, with food and water available *ad libitum*. Female mice were used because we are investigating the effect of pulmonary hypertension, a form of systemic hypoxia, which is more prevalent in females (Badesch et al., 2010; Benza et al., 2010; D'Alonzo et al., 1991). All efforts were made to minimize animal suffering, including the use of discarded animal carcasses for explorative procedures. For procedures that required anesthesia, animals were kept under supervision and warmed by a heat pad until they recovered.

2.2. Hypoxia model

We induced normobaric hypoxia in adult (6–8 weeks old) C57BL/6 female mice using a hypoxia chamber where animals were acclimated over 20 min from 20.9% to 10% oxygen as described previously (Sawada et al., 2014; Yuan et al., 2018). Mice were exposed to hypoxia for 48 h. Normoxic control mice were kept outside the chamber in the same animal facility.

2.3. Optical coherence tomography (OCT) and segmentation

To measure retinal structural changes over time, we performed spectral-domain optical coherence tomography (OCT) analysis using Spectralis™ HRA+OCT instrument (Heidelberg Engineering, GmbH, Heidelberg, Germany) (Ho et al., 2013; Shariati et al., 2015; Yu et al., 2014). Briefly, we dilated the eyes with 1% tropicamide (Alcon Laboratories, Inc., Fort Worth, TX) and 2.5% phenylephrine hydrochloride (Akorn, Inc., Lake Forest, IL) and covered the cornea with lubricating eye drops and custom-made contact lens (4 mm diameter). To measure retinal thickness, we performed a circular retinal nerve fiber layer (RNFL) scan around the optic nerve head and manually segmented total retinal thickness (TRT), which included RNFL to retinal pigmented epithelium (RPE) (Dysli et al., 2015), and the ganglion cell complex (GCC), which included RNFL to inner plexiform layer (INL) (Hein et al., 2012; Nakano et al., 2011). We computed the thickness of the INL-RPE layers by subtracting GCC from TRT (Fig. 1B). All segmentation was performed in a

Author Manuscript Author Manuscript Author Manuscript Author Manuscript

masked fashion, and every effort was made to standardize the segmentation process, which was performed by one well-trained individual and confirmed by a second investigator.

2.4. Tissue preparation and sectioning

Animals were deeply anesthetized and perfused through the heart with ice-cold saline followed by 4% paraformaldehyde in phosphate buffered saline (PBS). Eyes and optic nerves were removed, cryoprotected with 10–30% increasing sucrose gradient in PBS, and frozen in O.C.T. compound (Sakura Fineteck USA, Inc., Torrance, CA) with dry ice. Tissue blocks were sectioned using a cryostat into 12 μm thick slices and placed on frosted microscope glass slides (Fisher Scientific, Hampton, NH).

2.5. TUNEL assay

We performed Terminal deoxynucleotidyl transferase (TdT) dUTP Nick-End Labeling (TUNEL) assay for the detection of apoptosis in situ. The nucleotide-labeling mix was used in combination with the TUNEL enzyme to prepare a TUNEL reaction mixture (all from Sigma-Aldrich, city, State, USA) and the assay was performed according to the manufacturer's instructions. The number of TUNEL-positive cells was counted in 3-5 cross-sections of the retina (3-5 images acquired per retina up to 1 mm from the optic disc) and along the optic nerve. Results are expressed as the average number of TUNEL-positive cells per mm^2 ± SEM.

2.6. Retina and optic nerve analysis

Retinae and optic nerves were immunostained with primary antibodies to detect CHOP (1:50, mouse; catalog number MA1-250; Invitrogen, Waltham, MA, USA), glial fibrillary acidic protein (GFAP) (1:1000, chicken; catalog number ab4674; Abcam, Cambridge, MA, USA), myelin basic protein (MBP) (1:100, rat; catalog number MAB386, Millipore Sigma, Burlington, MA, USA), Iba1 (1:400, rabbit; catalog number 019-19741, Wako Chemicals, Richmond, VA, USA), Brn3a (1:500, goat; catalog number Sc-31984, Santa Cruz Biotechnology, Inc. Dallas, Texas, USA), Olig-2 (1: 200, rabbit; catalog number AB9610, Millipore Sigma, Burlington, MA, USA), CC-1 (1:20, mouse, catalog number OP80-100UG, Millipore Sigma), and PDGFRα (1:100, CD140a, rat; catalog number 558774, BD Biosciences, San Jose, CA, USA). Secondary antibodies used were Alexa 488 goat anti-mouse, Alexa 568 goat anti-chicken, Alexa 647 goat anti-rabbit, Alexa 568 goat anti-rat and Alexa 568 donkey anti-goat (all from Invitrogen Inc., Carlsbad, CA, USA). Slides were mounted using Vectashield with 4′,6-diamidino-2-phenylindole (DAPI) (Vector Laboratories, Burlingame, CA, USA). Sections were imaged under a Nikon Eclipse TE300 microscope (Nikon Corp., Tokyo, Japan) or a Zeiss inverted LSM 880 laser scanning confocal microscope (Carl Zeiss, Oberkochen, Germany).

2.7. Histology quantification of retinal thickness

To quantify the thickness of the retinal layers on histology, we imaged the DAPI-stained retinal slices and measured the thickness using ImageJ (http://rsbweb.nih.gov/ij/; provided in the public domain by the National Institutes of Health, Bethesda, MD, USA).

Author Manuscript Author Manuscript Author Manuscript Author Manuscript

We measured the thickness of the GCL to ONL (equivalent to total retinal thickness on OCT), GCL to IPL (equivalent to ganglion cell complex on OCT), and INL to ONL layers (equivalent to total retinal thickness minus ganglion cell complex) within 1.5 mm away from the optic nerve head. Each measurement was done in 3 locations per section and at least 3 sections per eye to calculate the average thickness.

2.8. Analysis of RGC survival

RGC survival was measured by the number of $Brn3a^+$ in retinal whole mount preparations. We took 4 images (four quadrants) in the center (~1 mm from the optic disc) and 4 images in the periphery (~2 mm from the optic disc) of the retina at magnification of 20x. We used the analyze particles tool of ImageJ to calculate the number of $Brn3A^+$cells per image automatically, averaged the number of cells in the center and periphery of each retina, and calculated the density of $Brn3A^+$ cells per mm^2. Each automatically performed cell count was visually reviewed under masked condition for quality control.

2.9. Fluorescence microscopy

For image quantification, we took standard images of the retinae and anterior optic nerve under masked condition with epifluorescence microscope using a 20x (numerical aperture 0.75) and 40x (numerical aperture 0.95) objective lenses. To standardize the region of interest of the retinae quantified, we acquired 3-5 images per retina using the same objective lens, located within 1.5 mm away from the optic nerve head. The region of interest was drawn for each image to outline all retinal layers from the RNFL to the ONL using the DAPI and GFAP channels as references.

For the optic nerve, we imaged horizontal optic nerve sections in the anterior optic nerve using same magnification and standardized parameters. To standardize the area of the optic nerve counted, we used MBP staining to determine the beginning of myelination as described previously (Yang et al., 2013) and performed measurements after drawing regions of interest covering the entire diameter of the optic nerve in four different segments per nerve (n0, n1, n2 and n3). The unmyelinated optic nerve was subdivided into n0 (totally inside the eye) and n1 (~125 μm along the optic nerve behind the outer nuclear layer of the retina), while the myelinated portion was subdivided into n2 (the transition from unmyelinated to myelinated, ~125 μm behind n1) and n3 (the myelinated anterior optic nerve, within ~300 μm after n2 ends).

2.10. Morphometric analysis of retina and optic nerve

All morphometric analyses were performed under masked condition. To quantify the fluorescence intensity associated to CHOP and GFAP expression, slides were immunostained at the same time and imaged using the same settings. For quantification, we used ImageJ to measure the mean gray value inside each region of interest. The results were expressed as arbitrary units (a.u.). To count $Iba1^+$ and oligodendroglia cells, the numbers of positive cells for Iba1, Olig2, CC-1 and PDGFRα were counted inside the region of interest in the retina or optic nerve and normalized by the area.

Author Manuscript Author Manuscript Author Manuscript Author Manuscript

2.11. Treatment with chemical chaperon 4-phenylbutyric acid in vivo

To assess the effect of chemical chaperon 4-phenylbutyric acid (4-PBA), we performed intraperitoneal injections of 4-PBA (40 mg/kg/day; 480 μl per injection) or vehicle (PBS). Animals were treated once a day with 4-PBA or PBS starting from 24 h before being placed in the hypoxia chamber to 24 h after being placed in the chamber.

2.12. Statistical analysis

We performed statistical analysis using the commercial statistical software Prism (GraphPad Inc., La Jolla, CA). We calculated statistical significance, which was defined as $p < 0.05$. We used *t*-test or Mann-Whitney test for all retina analyses and two-way ANOVA for comparisons including optic nerve segments and oligodendroglia subtypes. To correct for multiple comparisons, we used Sidak post-hoc test to compare optic nerve segments between experimental groups or Tukey post-hoc test to compare segments inside each group and to compare oligodendroglia subtypes. All data are presented as mean ± S.E.M.

3. Results

3.1. Hypoxia induced thinning of the retina on OCT but little cell loss on histology

After 48 h of hypoxia, optical coherence tomography (OCT) measurement revealed no changes in the ganglion cell complex (GCC) (baseline: 77.7 ± 0.6 μm, hypoxia: 78.3 ± 1.0 μm; P = 0.5333, paired *t*-test, n = 18), but a 5.1 μm reduction of the total retinal thickness (TRT) (RNFL to RPE) compared with baseline (baseline: 226.4 ± 1.5 μm, hypoxia: 221.3 ± 1.2 μm; P < 0.01, paired *t*-test, n = 18 eyes) (Fig. 1A-B). The reduced TRT was due to thinning in the layers of the retina from INL to RPE, which had 5.8 μm thinning (baseline: 148.7 ± 1.1, hypoxia: 142.9 ± 0.9 μm; P < 0.001, n = 18) (Fig. 1A-B).

To examine whether changes in thickness of the retinal layers after hypoxia were present histologically, we performed intracardiac perfusion as soon as possible after removing the animals from the hypoxia chamber, which was within 30 min for the first animal and within 2 h for the last animal. In hypoxia retinal sections stained with DAPI, the GCL to IPL thickness was not significantly different in hypoxia (control: 89.0 ± 6.8 μm, n = 7, hypoxia: 105.8 ± 2.4, n = 5, P = 0.1490, Mann-Whitney test), and there was no thinning of the GCL to ONL layer compared with controls (control: 267.7 ± 8.0 μm, n = 7, hypoxia: 290 ± 9.3, n = 5, P = 0.1061, Mann-Whitney test). There was a 5.6 μm reduction in the thickness from the INL to OPL, which was similar to OCT data, but this was not significant compared with controls (control: 179.9 ± 6.4 μm, n = 7, hypoxia: 174.3 ± 8.0, n = 5, P = 0.5303, Mann-Whitney test). Taken together, although there was some thinning of the INL to outer retinal layers on OCT, we did not see obvious explanation of this change on histology.

To see whether cell death was the reason for changes seen on OCT, we performed terminal deoxynucleotidyl transferase (TdT) dUTP nick-end labeling (TUNEL) stain. This revealed only rare $TUNEL^+$ cells in the retina (Fig. 2). In the retina, the $TUNEL^+$ cells were primarily located in the outer nuclear layer (Fig. 2A), with 1.5 ± 0.5 $TUNEL^+$ cells/mm^2 in the hypoxia group (n = 6) compared with 0.1 ± 0.1 in the control group (n = 4; P = 0.0429 Mann-Whitney). In addition, there were rare $TUNEL^+$ cells in the optic nerve (Fig. 2B). In

Author Manuscript Author Manuscript Author Manuscript Author Manuscript

the optic nerve, there was no difference in the number of TUNEL$^+$ cells between control (0.4 ± 0.3 cells/mm^2, n = 6) and hypoxia (0.1 ± 0.1 cells/mm^2, n = 6; P = 0.8485 Mann-Whitney).

Consistent with little TUNEL$^+$ cells in hypoxia group, quantification of Brn3a$^+$ RGCs in retinal whole mount preparations revealed no difference between the hypoxia and control groups (control: 2569 ± 168 cells/mm^2, n = 8; hypoxia: 2816 ± 67 cells/mm^2, n = 5; P = 0.2894, unpaired *t*-test, Fig. 2C-E). Thus, small changes in retinal thickness on OCT after hypoxia did not correspond to loss of neurons in the retina on histology.

3.2. Hypoxia increased CHOP expression in the retina and anterior optic nerve

Although there was little cell loss in the retina after 48 h of hypoxia, there was dramatic increase in the protein expression of proapoptotic transcriptional regulator CCAAT-enhancer-binding protein homologous protein (CHOP), a marker of cellular stress known to be significantly elevated in ischemic optic neuropathy (Kumar et al., 2019) and other experimental optic neuropathies (Doh et al., 2010; Hu et al., 2012; Huang et al., 2017). There was little CHOP immunoreactivity in control retina (Fig. 3A). Within 48 h of hypoxia, there was increased CHOP expression in all retinal neuronal layers (Fig. 3B). Morphometric analysis revealed that compared with control, hypoxia led to a significant, 26% increase in CHOP immunoreactivity in the retina (Fig. 3C; control: 661.7 ± 42.33 arbitrary units (a.u.), hypoxia: 839.9 ± 38.12 a.u., n ≥ 5, P < 0.05, unpaired *t*-test, Supplementary Table 1).

In the optic nerve, there was also little CHOP expression in control group (Fig. 3A'). After 48 h hypoxia, there was significant increase in CHOP expression in the optic nerve, and this increase was greatest in the unmyelinated portion of the optic nerve (Fig. 3B', C, I). To quantify changes in CHOP expression in different parts of the optic nerve, we divided the anterior optic nerve into the unmyelinated region, composed of intra-retinal (n0) and retro-bulbar (n1) portions, and the myelinated portion, composed of transition from unmyelinated to myelinated (n2) and myelinated proximal (n3) portions (Fig. 3I, also see Methods). CHOP expression was significantly increased in n0 to n2 but not n3 portions of the optic nerve (n0: P < 0.001, n ≥ 5; n1: P < 0.05, n ≥ 5; n2: P < 0.05, n ≥ 5; n3: P > 0.9999, n ≥ 5; two-way ANOVA with Sidak's multiple comparisons test) (Fig. 3C') (Supplementary Table 1). These findings showed that 48 h of hypoxia significantly increased CHOP expression in the retina and anterior optic nerve, consistent with increased cellular stress.

3.3. Hypoxia increased GFAP expression in the optic nerve but not retina

Given the increase in CHOP expression in the unmyelinated optic nerve, where astrocytes are abundant, we then quantified protein expression of glial fibrillary acidic protein (GFAP), which is associated with astrocyte reactivity (Clarke et al., 2018; Nichols et al., 1993). In the retina, there was no change in GFAP expression after hypoxia compared with controls (Fig. 3E, 3F). In contrast, the GFAP expression was increased in the optic nerve (Fig. 3E'). Quantification revealed that GFAP was significantly increased in n0-n2 but not n3 (n0: P < 0.001, n ≥ 5; n1: P < 0.01, n ≥ 5; n2 (P < 0.01, n ≥ 5; n3: P = 0.6531, n ≥ 5; two-way ANOVA with Sidak's multiple comparisons test) (Fig. 3F', Supplementary Table 1). This

Author Manuscript Author Manuscript Author Manuscript Author Manuscript

significant increase in CHOP and GFAP expression in unmyelinated optic nerve is consistent with astrocyte stress.

3.4. Hypoxia did not change the number of Iba1$^+$ cells in the retina and optic nerve

Since acute hypoxia is often associated with inflammation and microglial activation in the brain (Zhang et al., 2017; Zhou et al., 2017), we quantified the number of Iba1$^+$ cells in the retina and optic nerve. Quantification revealed that there was no significant difference in the number of cells between 48 h hypoxia and control in the retina and optic nerve (retina: $P = 0.4388$, $n \geq 5$; n0: $P = 0.6845$, $n \geq 5$; n1: $P = 0.5836$, $n \geq 5$; n2: $P = 0.1644$, $n \geq 5$; n3: $P = 0.7960$, $n \geq 5$, Supplementary Table 1).

3.5. Hypoxia led to significant reduction of total number of oligodendroglia in the optic nerve

Since oligodendrocytes have been shown to be selectively vulnerable to hypoxic-ischemic injury (Butt et al., 2017; Tekkok et al., 2007; Wang et al., 2018), we quantified the number of Olig2$^+$ optic nerve oligodendrocytes using immunohistochemistry. After 48 h hypoxia, there was significant, 9% reduction of Olig2$^+$ total population of oligodendrocytes (control: 1202.7 ± 32.3 Olig2$^+$ cells/mm^2, n = 8; hypoxia: 1095.8 ± 32.3, n = 10 $P < 0.05$, two-way ANOVA with Tukey's multiple comparisons test) (Fig. 4A, B, G). To investigate if hypoxia affected a specific stage of oligodendrocyte maturation, we counted the number of CC-1$^+$ (mature) and PDGFRα$^+$ (immature) cells. There was no significant change in the number of CC-1$^+$ (control: 1116.6 ± 27.9 CC-1$^+$ cells/mm^2, n = 9; hypoxia; 1044.2 ± 29.6, n = 10; $P = 0.1603$; two-way ANOVA with Tukey's multiple comparisons test) and PDGFRα$^+$ cells (control: 38.5 ± 8.2 PDGFRα$^+$ cells/mm^2, n = 3; hypoxia: 31.9 ± 4.6, n = 7; $P = 0.9930$; two-way ANOVA with Tukey's multiple comparisons test) (Fig. 4D, E, G).

3.6. Treatment with chemical chaperon 4-PBA rescued optic nerve oligodendrocytes

Given that chemical chaperon 4-PBA has been shown to ameliorate damage in experimental models of vision loss (Jeng et al., 2007; Jian et al., 2016; Mizukami et al., 2010; Srinivasan and Sharma, 2011; Tung et al., 2015; Zode et al., 2011, 2012, 2014), we pre-treated animals 24 h before and during 48 h hypoxia with intraperitoneal injections of chemical chaperone 4-PBA or vehicle (PBS). We found that 4-PBA treatment led to a significant, 12% increase of optic nerve Olig2$^+$ oligodendrocytes compared with PBS-treated hypoxic animals (PBS-treated hypoxia: 1095.8 ± 32.3 Olig2$^+$ cells/mm^2, n = 10 4-PBA-treated hypoxia: 1222.5 ± 32.7, n = 5; $P < 0.05$, two-way ANOVA with Tukey's multiple comparisons test) (Fig. 4C, G). The 4-PBA-treated hypoxia group had the same density of Olig2$^+$ cells in the optic nerve as naïve control eyes (naïve control: 1202.8 ± 32.3 Olig2$^+$ cells/mm^2, n = 8; $P = 0.9121$). Compared with PBS-treated hypoxia group, there was significant, 13% more CC-1$^+$ cells in 4-PBA-treated hypoxia group (PBS-treated hypoxia: 1044.2 ± 29.6 CC-1$^+$ cells/mm^2, n = 10; 4-PBA-treated hypoxia: 1184.6 ± 56.4, n = 5; $P < 0.05$; two-way ANOVA with Tukey's multiple comparisons test), but no difference in the number of PDGFRα$^+$ cells (PBS-treated hypoxia: 31.9 ± 4.6 PDGFRα$^+$ cells/mm^2, n = 7; 4-PBA-treated hypoxia: 33.4 ± 5.5, n = 4; $P = 0.9996$; two-way ANOVA with Tukey's multiple comparisons test) (Fig. 4D-G), consistent with 4-PBA protection of mature (CC-1$^+$) but not immature (PDGFRa$^+$) oligodendrocytes. Overall, our data showed that the optic nerve oligodendrocytes, but no

Author Manuscript Author Manuscript Author Manuscript Author Manuscript

other glial cells, were lost after 48 h hypoxia, and that 4-PBA pretreatment prevented oligodendroglia loss.

4. Discussion

We showed that 48 h hypoxia did not lead to immediate loss of RGCs, but that there was significant increase in the expression of CHOP, a proapoptotic transcription factor and marker of ER stress (Hu, 2016; Wang and Kaufman, 2016), in the RGC layer. In the optic nerve, CHOP expression was most striking in the unmyelinated portion, which corresponded with an increased GFAP expression, consistent with astrocyte reactivity. Although there was no immediate loss of RGCs after 48 h hypoxia, there was significant loss of $Olig2^+$ optic nerve oligodendrocytes, which are known to be vulnerable to hypoxic-ischemic injury (Butt et al., 2017; Tekkok et al., 2007; Wang et al., 2018), but not of $PDGFR\alpha^+$ immature oligodendrocytes, which are more resistant to hypoxia (Fern et al., 1998). This hypoxia-induced oligodendrocyte loss was completely salvaged by pre-treating the animals with chemical chaperon 4-PBA.

Taken together, our study delineated early cellular events that are consistent with the creation of a stress condition in the retina and optic nerve after systemic hypoxia (see model in Fig. 5). In normoxia, RGCs receive metabolic support from glia. Where RGC axons are unmyelinated, there is high metabolic demand due to passive conduction of action potentials, and *astrocytes* provide energy substrate for RGC axons (Marina et al., 2016; Sun et al., 2009). Where RGC axons are myelinated, there is essential support from oligodendrocytes (Lee et al., 2012; Nave, 2010) (Fig. 5A). We showed that after 48 h of hypoxia, there was evidence of astrocyte reactivity and loss of oligodendrocytes, which both impact RGC axons. We propose a model where astrocytes in the unmyelinated optic nerve sense hypoxia and respond by increasing ER stress and reactivity, leading to reduced metabolic support to RGC axons (Fig. 5B). Increased CHOP expression is associated with ER stress (Pereira et al., 2014) and is consistent with CHOP upregulation in retinal astrocytes in DBA/2 J glaucoma model (Ojino et al., 2015), after retina ischemia (Benavides et al., 2005; Lewis and Fisher, 2003) and in Muller cells of diabetic rats (Sanchez-Chavez et al., 2016). Although sustained CHOP expression is associated with astrocyte death (Benavides et al., 2005; Ojino et al., 2015; Zinszner et al., 1998), we have not found evidence of astrocyte death after systemic hypoxia, since no $TUNEL^+$ cells were found in the inner retinal layers and in the anterior optic nerve. Since GFAP upregulation is associated with astrocyte reactivity (Clarke et al., 2018; Nichols et al., 1993), increased CHOP expression in $GFAP^+$ cells can also mean a specific type of astrocyte activation. For instance, hypobaric hypoxia increases proteins from the complement cascade in the hippocampus (Dheer et al., 2018), which are typical from toxic activation phenotypes (Liddelow et al., 2017), but further studies are needed to identify whether or not they are specific to astrocyte activation.

Similarly, oligodendrocyte loss in the myelinated optic nerve may impair the support to RGC axons in the myelinated optic nerve (Fig. 5C) (Lee et al., 2012), since mature oligodendrocytes are highly vulnerable to hypoxia (Butt et al., 2017; Tekkok et al., 2007; Wang et al., 2018). Indeed, loss of $Olig2^+$ oligodendrocytes within 48 h hypoxia suggests

Author Manuscript Author Manuscript Author Manuscript Author Manuscript

that oligodendrocyte death occurred rapidly, which is consistent with early loss of myelin in the hippocampus after hypobaric hypoxia (Dheer et al., 2018; Zhang et al., 2017) and after experimental anterior ischemic optic neuropathy (Goldenberg-Cohen et al., 2005; Pangratz-Fuehrer et al., 2011). Although the exact mechanism of oligodendrocyte loss is unclear, oligodendrocytes are vulnerable to energy failure because of their high metabolic demand for protein and lipid synthesis (Clayton and Popko, 2016; D'Antonio et al., 2009), and because their glutamate receptors can be excessively activated when glutamate accumulates in the extracellular space as a result of hypoxic-ischemic insult (Matute et al., 2013). In addition, since the adult optic nerve keeps generating new oligodendrocytes to replace oligodendrocytes that die in service (Young et al., 2013), it is possible that hypoxia impairs this physiological process, resulting in a decrease of total oligodendrocytes. In the short-term, loss of oligodendrocytes can mean temporary loss of visual function without losing any RGCs or axons. In the long-term, loss of oligodendrocytes likely contributes to degeneration of the RGCs, since 99% of the optic nerve axons are covered in myelin and, without enough contact to the extracellular space, these RGC axons are heavily dependent on lactate from oligodendrocytes as an energy source (Baltan, 2015; Hirrlinger and Nave, 2014; Lee et al., 2012; Nave, 2010; Rinholm and Bergersen, 2014).

While hypoxia led to oligodendrocyte loss, pre-treatment with 4-PBA rescued the optic nerve oligodendrocytes. However, the mechanisms that led to oligodendrocyte protection are unclear, since 4-PBA is a molecule with multiple effects. For instance, 4-PBA is thought to act as a chemical chaperon and reduced ER stress on mouse neurons after ischemic/reperfusion injury (Mizukami et al., 2010; Srinivasan and Sharma, 2011), in glaucomatous trabecular meshwork (Tung et al., 2015; Zode et al., 2011, 2014), and in human neuronal cells after oxygen-glucose deprivation and reoxygenation in vitro (Tung et al., 2015). In addition to reducing ER stress, 4-PBA has also been described to act as a histone deacetylase inhibitor (Kusaczuk et al., 2015), which is associated to oligodendrocyte protection (Egawa et al., 2019; Wang et al., 2015). Chemical chaperons like 4-PBA are already in routine clinical use as they are Food and Drug Administration-approved for the treatment of hyperammonia, urea cycle abnormality and cystic fibrosis (Iannitti and Palmieri, 2011; Schonthal, 2012). Since 4-PBA treatment salvaged neurons in preclinical studies (Zode et al., 2011, 2014), it is a potential repurposable drug to treat CNS hypoxic-ischemic disease. Consistent with the effects of 4-PBA in oligodendrocyte survival after hypoxia, 4-PBA significantly preserved both $Brn3A^+$ RGCs and $Olig2^+$ oligodendrocytes after experimental anterior ischemic optic neuropathy (Kumar et al., 2019). Therefore, although neuroprotective therapies have primarily focused on saving RGC soma and axons (Kumar et al., 2019), our study provided evidence that glia-directed therapies (Mesentier-Louro et al., 2018a,b; Mesentier-Louro and Liao, 2019) may be a novel approach in the treatment of systemic hypoxia.

Limitations to our study include the difficulty of comparing in vivo retinal thickness measured by OCT with histology. In addition, although we showed that there was increased CHOP in the retina and optic nerve and 4-PBA rescued oligodendrocytes, we did not show that this was due to ER stress. We did find that CHOP expression is a useful marker of cellular stress in the retina and optic nerve after hypoxia, as it is in the retina after glaucoma (Ojino et al., 2015), ischemia (Benavides et al., 2005; Lewis and Fisher, 2003) and diabetes

Author Manuscript Author Manuscript Author Manuscript Author Manuscript

(Sanchez-Chavez et al., 2016). Although we did not investigate changes after different durations of hypoxic exposure, our data show that this murine model is a good way to further study the effects of hypoxia on the visual system. Nevertheless, our results reflect only immediate/early changes after hypoxia exposure, and studies at longer exposure times may be performed to understand the impact on neurons and glia in the visual system.

5. Conclusion

Forty-eight-hour hypoxia has differential impact on neurons and glial cells in the retina and optic nerve, with more impact on the glia than RGCs. We conclude that astrocyte stress and loss of oligodendroglia in the optic nerve reflect a selective vulnerability of the visual system to systemic hypoxia. Glial-protective therapies may be a novel approach in hypoxic-ischemic injury by protecting the white matter and potentially preserving vision.

Supplementary Material

Refer to Web version on PubMed Central for supplementary material.

Acknowledgments

We thank Dr. Yang Hu for his help with ER stress pathway, Dr. Ke Yuan and Abinaya Nathan for help with hypoxia animal model, Matthew E. Dardet for help with morphometric analysis, Annie T. Nguyen and Palak Patel for proof-reading the manuscript, and Dr Evan Cameron for critical advice.

Financial disclosure

Y.J.L. was supported by North American Neuro-Ophthalmology Society Pilot Grant, Stanford Vice Provost for Undergraduate Education Grant, Stanford Diabetes Research Center Pilot Grant, National Eye Institute (P30-026877) and Research to Prevent Blindness, Inc. L.A.M.L was supported by Stanford TRAM Pilot Grant. V.D.J.P. was supported by grants from the NIH (R01 R01HL139664, PI, 9/1/2017-8/30/2021, Role of Wnt5a in endothelial-pericyte interactions in the lung; R01 HL134776, PI, 1/1/2017-12/30/2022, Wnt7a/ROR2 in the heart and lung).

Abbreviations:

4-PBA	4-phenylbutyric acid
CHOP	CCAAT-enhancer-binding protein homologous protein
ER	endoplasmic reticulum
CNS	central nervous system
GCC	ganglion cell complex
GFAP	glial fibrillary acidic protein
OCT	optical coherence tomography
ONL	outer nuclear layer
RGC	retinal ganglion cell
TRT	total retinal thickness

Author Manuscript Author Manuscript Author Manuscript Author Manuscript

TUNEL terminal deoxynucleotidyl transferase dUTP nick end labeling

References

Arjamaa O, Nikinmaa M, 2006 Oxygen-dependent diseases in the retina: role of hypoxia-inducible factors. Exp. Eye Res 83, 473–483. [PubMed: 16750526]

Badesch DB, Raskob GE, Elliott CG, Krichman AM, Farber HW, Frost AE, Barst RJ, Benza RL, Liou TG, Turner M, Giles S, Feldkircher K, Miller DP, McGoon MD, 2010 Pulmonary arterial hypertension: baseline characteristics from the REVEAL Registry. Chest 137, 376–387. [PubMed: 19837821]

Baltan S, 2015 Can lactate serve as an energy substrate for axons in good times and in bad, in sickness and in health? Metab. Brain Dis 30, 25–30. [PubMed: 25034458]

Bandyopadhyay S, Singh R, Gupta V, Gupta A, 2002 Anterior ischaemic optic neuropathy at high altitude. Indian J. Ophthalmol 50, 324–325. [PubMed: 12532501]

Benavides A, Pastor D, Santos P, Tranque P, Calvo S, 2005 CHOP plays a pivotal role in the astrocyte death induced by oxygen and glucose deprivation. Glia 52, 261–275. [PubMed: 16001425]

Benza RL, Miller DP, Gomberg-Maitland M, Frantz RP, Foreman AJ, Coffey CS, Frost A, Barst RJ, Badesch DB, Elliott CG, Liou TG, McGoon MD, 2010 Predicting survival in pulmonary arterial hypertension: insights from the registry to evaluate early and long-term pulmonary arterial hypertension disease management (REVEAL). Circulation 122, 164–172. [PubMed: 20585012]

Bosch MM, Barthelmes D, Landau K, 2012 High altitude retinal hemorrhages–an update. High Alt. Med. Biol 13, 240–244. [PubMed: 23270439]

Butt AM, Vanzulli I, Papanikolaou M, De La Rocha IC, Hawkins VE, 2017 Metabotropic glutamate receptors protect oligodendrocytes from acute ischemia in the mouse optic nerve. Neurochem. Res 42, 2468–2478. [PubMed: 28365868]

Caprara C, Grimm C, 2012 From oxygen to erythropoietin: relevance of hypoxia for retinal development, health and disease. Prog. Retin. Eye Res 31, 89–119. [PubMed: 22108059]

Clarke LE, Liddelow SA, Chakraborty C, Munch AE, Heiman M, Barres BA, 2018 Normal aging induces A1-like astrocyte reactivity. Proc. Natl. Acad. Sci. U. S. A 115, E1896–E1905. [PubMed: 29437957]

Clayton BLL, Popko B, 2016 Endoplasmic reticulum stress and the unfolded protein response in disorders of myelinating glia. Brain Res. 1648, 594–602. [PubMed: 27055915]

D'Alonzo GE, Barst RJ, Ayres SM, Bergofsky EH, Brundage BH, Detre KM, Fishman AP, Goldring RM, Groves BM, Kernis JT, et al., 1991 Survival in patients with primary pulmonary hypertension. Results from a national prospective registry. Ann. Intern. Med 115, 343–349. [PubMed: 1863023]

D'Antonio M, Feltri ML, Wrabetz L, 2009 Myelin under stress. J. Neurosci. Res 87, 3241–3249. [PubMed: 19330777]

Dheer A, Jain V, Kushwah N, Kumar R, Prasad D, Singh SB, 2018 Temporal and spatial changes in glial cells during chronic hypobaric hypoxia: role in neurodegeneration. Neuroscience 383, 235–246. [PubMed: 29751055]

Doh SH, Kim JH, Lee KM, Park HY, Park CK, 2010 Retinal ganglion cell death induced by endoplasmic reticulum stress in a chronic glaucoma model. Brain Res. 1308, 158–166. [PubMed: 19853589]

Drel VR, Xu W, Zhang J, Kador PF, Ali TK, Shin J, Julius U, Slusher B, El-Remessy AB, Obrosova IG, 2009 Poly(ADP-ribose)polymerase inhibition counteracts cataract formation and early retinal changes in streptozotocin-diabetic rats. Invest. Ophthalmol. Vis. Sci 50, 1778–1790. [PubMed: 19098320]

Dysli C, Enzmann V, Sznitman R, Zinkernagel MS, 2015 Quantitative analysis of mouse retinal layers using automated segmentation of spectral domain optical coherence tomography images. Transl. Vis. Sci. Technol 4, 9.

Egawa N, Shindo A, Hikawa R, Kinoshita H, Liang AC, Itoh K, Lok J, Maki T, Takahashi R, Lo EH, Arai K, 2019 Differential roles of epigenetic regulators in the survival and differentiation of oligodendrocyte precursor cells. Glia 67, 718–728. [PubMed: 30793389]

Author Manuscript Author Manuscript Author Manuscript Author Manuscript

Fern R, Davis P, Waxman SG, Ransom BR, 1998 Axon conduction and survival in CNS white matter during energy deprivation: a developmental study. J. Neurophysiol 79, 95–105. [PubMed: 9425180]

Ferriero DM, 2004 Neonatal brain injury. N. Engl. J. Med 351, 1985–1995. [PubMed: 15525724]

Goldenberg-Cohen N, Guo Y, Margolis F, Cohen Y, Miller NR, Bernstein SL, 2005 Oligodendrocyte dysfunction after induction of experimental anterior optic nerve ischemia. Invest. Ophthalmol. Vis. Sci 46, 2716–2725. [PubMed: 16043843]

Guduru A, Martz TG, Waters A, Kshirsagar AV, Garg S, 2016 Oxygen saturation of retinal vessels in all stages of diabetic retinopathy and correlation to ultra-wide field fluorescein angiography. Invest. Ophthalmol. Vis. Sci 57, 5278–5284. [PubMed: 27723894]

Hartnett ME, Penn JS, 2012 Mechanisms and management of retinopathy of prematurity. N. Engl. J. Med 367, 2515–2526. [PubMed: 23268666]

Hein K, Gadjanski I, Kretzschmar B, Lange K, Diem R, Sattler MB, Bahr M, 2012 An optical coherence tomography study on degeneration of retinal nerve fiber layer in rats with autoimmune optic neuritis. Investig. Ophthalmol. Vis. Sci 53, 157–163. [PubMed: 22131393]

Hirrlinger J, Nave KA, 2014 Adapting brain metabolism to myelination and long-range signal transduction. Glia 62, 1749–1761. [PubMed: 25130164]

Ho JK, Stanford M, Shariati MA, Dalal R, Liao YJ, 2013 Optical coherence tomography study of experimental anterior ischemic optic neuropathy and histologic confirmation. Investig. Ophthalmol. Vis. Sci 54, 5981–5988. [PubMed: 23887804]

Hu Y, 2016 Axon injury induced endoplasmic reticulum stress and neurodegeneration. Neural Regen. Res 11, 1557–1559. [PubMed: 27904477]

Hu Y, Park KK, Yang L, Wei X, Yang Q, Cho KS, Thielen P, Lee AH, Cartoni R, Glimcher LH, Chen DF, He Z, 2012 Differential effects of unfolded protein response pathways on axon injury-induced death of retinal ganglion cells. Neuron 73, 445–452. [PubMed: 22325198]

Huang H, Miao L, Liang F, Liu X, Xu L, Teng X, Wang Q, Ridder WH 3rd, Shindler KS, Sun Y, Hu Y, 2017 Neuroprotection by eIF2alpha-CHOP inhibition and XBP-1 activation in EAE/optic neuritiss. Cell Death Dis. 8, e2936. [PubMed: 28726788]

Iannitti T, Palmieri B, 2011 Clinical and experimental applications of sodium phenylbutyrate. Drugs R 11, 227–249.

Jeng YY, Lin NT, Chang PH, Huang YP, Pang VF, Liu CH, Lin CT, 2007 Retinal ischemic injury rescued by sodium 4-phenylbutyrate in a rat model. Exp. Eye Res 84, 486–492. [PubMed: 17178414]

Jha MK, Morrison BM, 2018 Glia-neuron energy metabolism in health and diseases: new insights into the role of nervous system metabolic transporters. Exp. Neurol 309, 23–31. [PubMed: 30044944]

Jian L, Lu Y, Lu S, Lu C, 2016 Chemical chaperone 4-pheny[butyric acid protects H9c2 cardiomyocytes from ischemia/reperfusion injury by attenuating endoplasmic reticulum stress-induced apoptosis. Mol. Med. Rep 13, 4386–4392. [PubMed: 27035223]

Kaur C, Foulds WS, Ling EA, 2008 Hypoxia-ischemia and retinal ganglion cell damage. Clin. Ophthalmol 2, 879–889. [PubMed: 19668442]

Kergoat H, Herard ME, Lemay M, 2006 RGC sensitivity to mild systemic hypoxia. Invest. Ophthalmol. Vis. Sci 47, 5423–5427. [PubMed: 17122132]

Kumar V, Mesentier-Louro LA, Oh AJ, Heng K, Shariati MA, Huang H, Hu Y, Liao YJ, 2019 Increased ER stress after experimental ischemic optic neuropathy and improved RGC and oligodendrocyte survival after treatment with chemical chaperon. Invest. Ophthalmol. Vis. Sci 60, 1953–1966. [PubMed: 31060051]

Kusaczuk M, Bartoszewicz M, Cechowska-Pasko M, 2015 Phenylbutyric Acid: simple structure - multiple effects. Curr. Pharmaceut. Des 21, 2147–2166.

Lee Y, Morrison BM, Li Y, Lengacher S, Farah MH, Hoffman PN, Liu Y, Tsingalia A, Jin L, Zhang PW, Pellerin L, Magistretti PJ, Rothstein JD, 2012 Oligodendroglia metabolically support axons and contribute to neurodegeneration. Nature 487, 443–448. [PubMed: 22801498]

Lewis GP, Fisher SK, 2003 Up-regulation of glial fibrillary acidic protein in response to retinal injury: its potential role in glial remodeling and a comparison to vimentin expression. Int. Rev. Cytol 230, 263–290. [PubMed: 14692684]

Author Manuscript Author Manuscript Author Manuscript Author Manuscript

Li J, Wang JJ, Yu Q, Wang M, Zhang SX, 2009 Endoplasmic reticulum stress is implicated in retinal inflammation and diabetic retinopathy. FEBS Lett. 583, 1521–1527. [PubMed: 19364508]

Liddelow SA, Guttenplan KA, Clarke LE, Bennett FC, Bohlen CJ, Schirmer L, Bennett ML, Munch AE, Chung WS, Peterson TC, Wilton DK, Frouin A, Napier BA, Panicker N, Kumar M, Buckwalter MS, Rowitch DH, Dawson VL, Dawson TM, Stevens B, Barres BA, 2017 Neurotoxic reactive astrocytes are induced by activated microglia. Nature 541, 481–487. [PubMed: 28099414]

Linsenmeier RA, Zhang HF, 2017 Retinal oxygen: from animals to humans. Prog. Retin. Eye Res 58, 115–151. [PubMed: 28109737]

Marina N, Kasymov V, Ackland GL, Kasparov S, Gourine AV, 2016 Astrocytes and brain hypoxia. Adv. Exp. Med. Biol 903, 201–207. [PubMed: 27343098]

Matute C, Domercq M, Perez-Samartin A, Ransom BR, 2013 Protecting white matter from stroke injury. Stroke 44, 1204–1211. [PubMed: 23212168]

Mesentier-Louro LA, Dodd R, Domizi P, Nobuta H, Wernig M, Wernig G, Liao YJ, 2018a Direct targeting of the mouse optic nerve for therapeutic delivery. J. Neurosci. Methods 313, 1–5. [PubMed: 30389488]

Mesentier-Louro LA, Liao YJ, 2019 Optic nerve regeneration: considerations on treatment of acute optic neuropathy and end-stage disease. Curr. Ophthalmol. Rep 7, 11–20.

Mesentier-Louro LA, Rosso P, Carito V, Mendez-Otero R, Santiago MF, Rama P, Lambiase A, Tirassa P, 2018b Nerve growth factor role on retinal ganglion cell survival and axon regrowth: effects of ocular administration in experimental model of optic nerve injury. Mol. Neurobiol 56, 1056–1069. [PubMed: 29869196]

Mizukami T, Orihashi K, Herlambang B, Takahashi S, Hamaishi M, Okada K, Sueda T, 2010 Sodium 4-phenylbutyrate protects against spinal cord ischemia by inhibition of endoplasmic reticulum stress. J. Vase. Surg 52, 1580–1586.

Nakano N, Ikeda HO, Hangai M, Muraoka Y, Toda Y, Kakizuka A, Yoshimura N, 2011 Longitudinal and simultaneous imaging of retinal ganglion cells and inner retinal layers in a mouse model of glaucoma induced by N-methyl-D-aspartate. Investig. Ophthalmol. Vis. Sci 52, 8754–8762. [PubMed: 22003119]

Nave KA, 2010 Myelination and support of axonal integrity by glia. Nature 468, 244–252. [PubMed: 21068833]

Nichols NR, Day JR, Laping NJ, Johnson SA, Finch CE, 1993 GFAP mRNA increases with age in rat and human brain. Neurobiol. Aging 14, 421–429. [PubMed: 8247224]

Ojino K, Shimazawa M, Izawa H, Nakano Y, Tsuruma K, Hara H, 2015 Involvement of endoplasmic reticulum stress in optic nerve degeneration after chronic high intraocular pressure in DBA/2J mice. J. Neurosci. Res 93, 1675–1683. [PubMed: 26271210]

Oshitari T, Yoshida-Hata N, Yamamoto S, 2010 Effect of neurotrophic factors on neuronal apoptosis and neurite regeneration in cultured rat retinas exposed to high glucose. Brain Res. 1346, 43–51. [PubMed: 20573599]

Oshitari T, Yoshida-Hata N, Yamamoto S, 2011 Effect of neurotrophin-4 on endoplasmic reticulum stress-related neuronal apoptosis in diabetic and high glucose exposed rat retinas. Neurosci. Lett 501, 102–106. [PubMed: 21767604]

Pangratz-Fuehrer S, Kaur K, Ousman SS, Steinman L, Liao YJ, 2011 Functional rescue of experimental ischemic optic neuropathy with alphaB-crystallin. Eye 25, 809–817. [PubMed: 21475310]

Pereira ER, Frudd K, Awad W, Hendershot LM, 2014 Endoplasmic reticulum (ER) stress and hypoxia response pathways interact to potentiate hypoxia-inducible factor 1 (HIF-1) transcriptional activity on targets like vascular endothelial growth factor (VEGF). J. Biol. Chem 289, 3352–3364. [PubMed: 24347168]

Qi X, Hosoi T, Okuma Y, Kaneko M, Nomura Y, 2004 Sodium 4-phenylbutyrate protects against cerebral ischemic injury. Mol. Pharmacol 66, 899–908. [PubMed: 15226415]

Rinholm JE, Bergersen LH, 2014 White matter lactate–does it matter? Neuroscience 276, 109–116. [PubMed: 24125892]

Author Manuscript Author Manuscript Author Manuscript Author Manuscript

Sanchez-Chavez G, Hernandez-Ramirez E, Osorio-Paz I, Hernandez-Espinosa C, Salceda R, 2016 Potential role of endoplasmic reticulum stress in pathogenesis of diabetic retinopathy. Neurochem. Res 41, 1098–1106. [PubMed: 26721508]

Sawada H, Saito T, Nickel NP, Alastalo TP, Glotzbach JP, Chan R, Haghighat L, Fuchs G, Januszyk M, Cao A, Lai YJ, Perez Vde J, Kim YM, Wang L, Chen PI, Spiekerkoetter E, Mitani Y, Gurtner GC, Sarnow P, Rabinovitch M, 2014 Reduced BMPR2 expression induces GM-CSF translation and macrophage recruitment in humans and mice to exacerbate pulmonary hypertension. J. Exp. Med 211, 263–280. [PubMed: 24446489]

Schatz A, Guggenberger V, Fischer MD, Schommer K, Bartz-Schmidt KU, Gekeler F, Willmann G, 2018 Optic nerve oedema at high altitude occurs independent of acute mountain sickness. Br. J. Ophthalmol 103.

Schonthal AH, 2012 Endoplasmic reticulum stress: its role in disease and novel prospects for therapy. Scientifica (Cairo) 2012, 857516. [PubMed: 24278747]

Shariati MA, Park JH, Liao YJ, 2015 Optical coherence tomography study of retinal changes in normal aging and after ischemia. Investig. Ophthalmol. Vis. Sci 56, 2790–2797. [PubMed: 25414186]

Shimazawa M, Miwa A, Ito Y, Tsuruma K, Aihara M, Hara H, 2012 Involvement of endoplasmic reticulum stress in optic nerve degeneration following N-methyl-D-aspartate-induced retinal damage in mice. J. Neurosci. Res 90, 1960–1969. [PubMed: 22674348]

Srinivasan K, Sharma SS, 2011 Sodium phenylbutyrate ameliorates focal cerebral ischemic/reperfusion injury associated with comorbid type 2 diabetes by reducing endoplasmic reticulum stress and DNA fragmentation. Behav. Brain Res 225, 110–116. [PubMed: 21767572]

Sun D, Lye-Barthel M, Masland RH, Jakobs TC, 2009 The morphology and spatial arrangement of astrocytes in the optic nerve head of the mouse. J. Comp. Neurol 516, 1–19. [PubMed: 19562764]

Tekkok SB, Ye Z, Ransom BR, 2007 Excitotoxic mechanisms of ischemic injury in myelinated white matter. J. Cerebr. Blood Flow Metabol 27, 1540–1552.

Tezel G, Wax MB, 2004 Hypoxia-inducible factor 1alpha in the glaucomatous retina and optic nerve head. Arch. Ophthalmol 122, 1348–1356. [PubMed: 15364715]

Tian X, Zhang B, Jia Y, Wang C, Li Q, 2018 Retinal changes following rapid ascent to a high-altitude environment. Eye 32, 370–374. [PubMed: 28912514]

Tung WF, Chen WJ, Hung HC, Liu GY, Tung JN, Huang CC, Lin CL, 2015 4-Phenylbutyric acid (4-PBA) and lithium cooperatively attenuate cell death during oxygen-glucose deprivation (OGD) and reoxygenation. Cell. Mol. Neurobiol 35, 849–859. [PubMed: 25776137]

Wang F, Yang YJ, Yang N, Chen XJ, Huang NX, Zhang J, Wu Y, Liu Z, Gao X, Li T, Pan GQ, Liu SB, Li HL, Fancy SPJ, Xiao L, Chan JR, Mei F, 2018 Enhancing oligodendrocyte myelination rescues synaptic loss and improves functional recovery after chronic hypoxia. Neuron 99, 689–701 e685. [PubMed: 30078577]

Wang G, Shi Y, Jiang X, Leak RK, Hu X, Wu Y, Pu H, Li WW, Tang B, Wang Y, Gao Y, Zheng P, Bennett MV, Chen J, 2015 HDAC inhibition prevents white matter injury by modulating microglia/macrophage polarization through the GSK3beta/PTEN/Akt axis. Proc. Natl. Acad. Sci. U. S. A 112 2853–2858. [PubMed: 25691750]

Wang M, Kaufman RJ, 2016 Protein misfolding in the endoplasmic reticulum as a conduit to human disease. Nature 529, 326–335. [PubMed: 26791723]

Wangsa-Wirawan ND, Linsenmeier RA, 2003 Retinal oxygen: fundamental and clinical aspects. Arch. Ophthalmol 121, 547–557. [PubMed: 12695252]

Yang X, Zou H, Jung G, Richard G, Linke SJ, Ader M, Bartsch U, 2013 Nonneuronal control of the differential distribution of myelin along retinal ganglion cell axons in the mouse. Invest. Ophthalmol. Vis. Sci 54, 7819–7827. [PubMed: 24222305]

Young KM, Psachoulia K, Tripathi RB, Dunn SJ, Cossell L, Attwell D, Tohyama K, Richardson WD, 2013 Oligodendrocyte dynamics in the healthy adult CNS: evidence for myelin remodeling. Neuron 77, 873–885. [PubMed: 23473318]

Yu CH, K J, Liao YJ, 2014 Subretinal fluid is common in experimental non-arteritic anterior ischemic optic neuropathy. Eye 28, 1494–1501. [PubMed: 25257770]

Yuan K, Shamskhou EA, Orcholski ME, Nathan A, Reddy S, Honda H, Mani V, Zeng Y, Ozen MO, Wang L, Demirci U, Tian W, Nicolls MR, de Jesus Perez VA, 2018 Loss of endothelial derived

Author Manuscript Author Manuscript Author Manuscript Author Manuscript

WNT5A is associated with reduced pericyte recruitment and small vessel loss in pulmonary arterial hypertension. Circulation 139, 1710–1724.

Zhang F, Zhong R, Li S, Fu Z, Cheng C, Cai H, Le W, 2017 Acute hypoxia induced an imbalanced M1/M2 activation of microglia through NF-kappaB signaling in alzheimer's disease mice and wild-type littermates. Front. Aging Neurosci 9, 282. [PubMed: 28890695]

Zhou Y, Huang X, Zhao T, Qiao M, Zhao X, Zhao M, Xu L, Zhao Y, Wu L, Wu K, Chen R, Fan M, Zhu L, 2017 Hypoxia augments LPS-induced inflammation and triggers high altitude cerebral edema in mice. Brain Behav. Immun 64, 266–275. [PubMed: 28433745]

Zinszner H, Kuroda M, Wang X, Batchvarova N, Lightfoot RT, Remotti H, Stevens JL, Ron D, 1998 CHOP is implicated in programmed cell death in response to impaired function of the endoplasmic reticulum. Genes Dev. 12, 982–995. [PubMed: 9531536]

Zode GS, Bugge KE, Mohan K, Grozdanic SD, Peters JC, Koehn DR, Anderson MG, Kardon RH, Stone EM, Sheffield VC, 2012 Topical ocular sodium 4-phenylbutyrate rescues glaucoma in a myocilin mouse model of primary open-angle glaucoma. Invest. Ophthalmol. Vis. Sci 53, 1557–1565. [PubMed: 22328638]

Zode GS, Kuehn MH, Nishimura DY, Searby CC, Mohan K, Grozdanic SD, Bugge K, Anderson MG, Clark AF, Stone EM, Sheffield VC, 2011 Reduction of ER stress via a chemical chaperone prevents disease phenotypes in a mouse model of primary open angle glaucoma. J. Clin. Invest 121, 3542–3553. [PubMed: 21821918]

Zode GS, Sharma AB, Lin X, Searby CC, Bugge K, Kim GH, Clark AF, Sheffield VC, 2014 Ocular-specific ER stress reduction rescues glaucoma in murine glucocorticoid-induced glaucoma. J. Clin. Invest 124, 1956–1965. [PubMed: 24691439]

Author Manuscript Author Manuscript Author Manuscript Author Manuscript

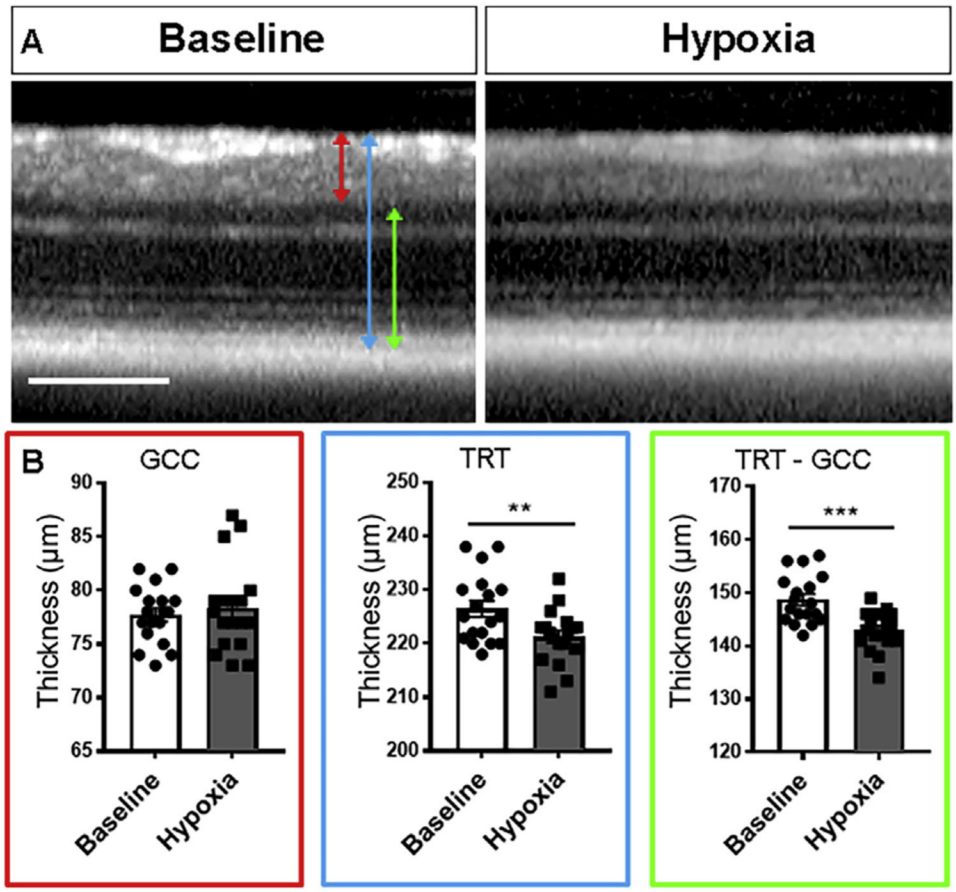

Fig. 1. No change in ganglion cell complex after 48h hypoxia.

A: High magnification of circle scans acquired using optical coherence tomography in vivo imaging before and after 48 h hypoxia. **B:** Bar graph of retinal thickness before and after hypoxia. Red line: ganglion cell complex (GCC); blue line: total retinal thickness (TRT); green line: TRT minus GCC. Scale bar: 200 µm.

Author Manuscript Author Manuscript Author Manuscript Author Manuscript

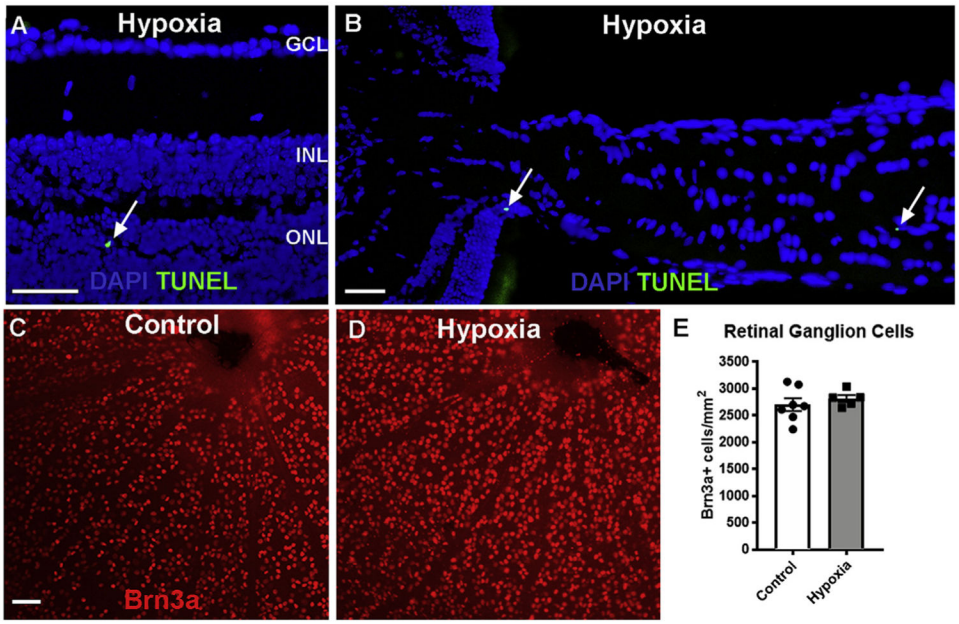

Fig. 2. Hypoxia led to little cell loss in the retina and optic nerve.

A-B: TUNEL staining (green, arrows) of a cross-section of retina (A) and optic nerve (B) after 48 h hypoxia. DAPI (blue) labeled nuclei. **C-D:** Retinal whole mount preparation of control and 48 h hypoxia eyes immunostained for Brn3a (red). **E:** bar graph of quantification of $Brn3a^+$ cells in the retina of control and 48 h hypoxia groups. P = 0.2894 (unpaired *t*-test). Scale bar: 100 μm. GCL: ganglion cell layer; INL: inner nuclear layer; ONL: outer nuclear layer.

Author Manuscript Author Manuscript Author Manuscript Author Manuscript

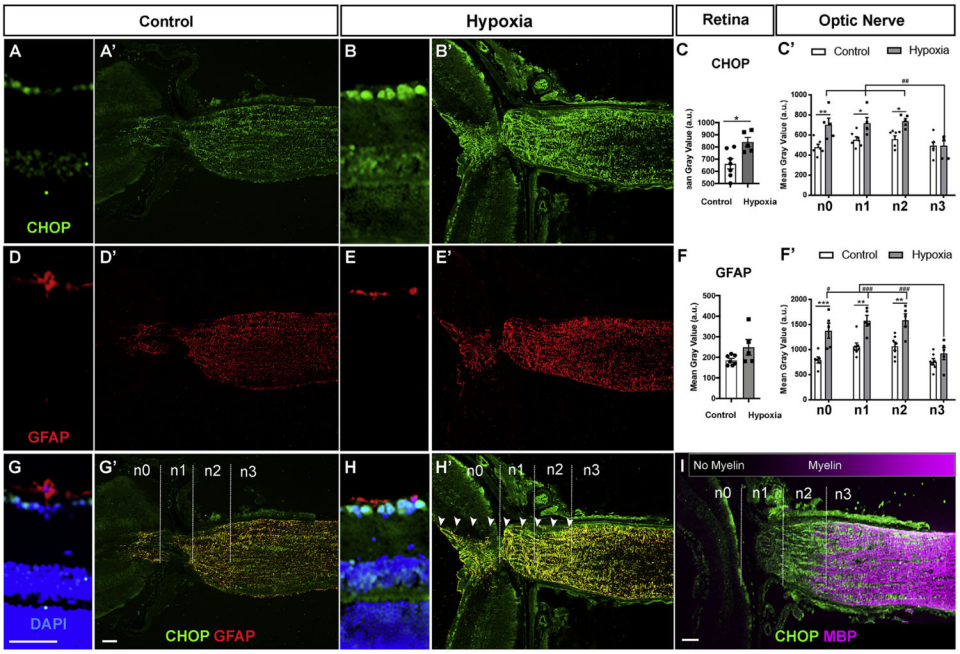

Fig. 3. Hypoxia led to significant increase in CHOP and GFAP expression in the anterior optic nerve.

A-I: Immunostaining for CHOP (A-B) and GFAP (D-E) immunostaining in the retina (A, B, D, E) and optic nerve (A′, B′, D′, E′). **C, F:** Bar graphs of CHOP (C, C′) and GFAP (F, F′) fluorescence intensities (Mean Gray Value) in the retina (C, F) and n0 to n3 optic nerve segments (C′, F′). **G-I:** Merged images and optic nerve segments (n0-n3). Nuclei in G and H were stained with DAPI (blue). Arrowheads indicate co-localization of CHOP and GFAP in the n0, n1 and n2 segments. **I:** CHOP distribution in unmyelinated versus myelinated optic nerve is shown by co-staining with myelin basic protein (MBP). *P < 0.05, **P < 0.01, ***P < 0.001 (unpaired *t*-test for retinas, two-way ANOVA with Sidaks's multiple comparisons test for optic nerve); #P < 0.05, ##P < 0.01, ###P < 0.001 (two-way ANOVA with Tukey's multiple comparisons test). Scale bar: 100 μm.

Author Manuscript Author Manuscript Author Manuscript Author Manuscript

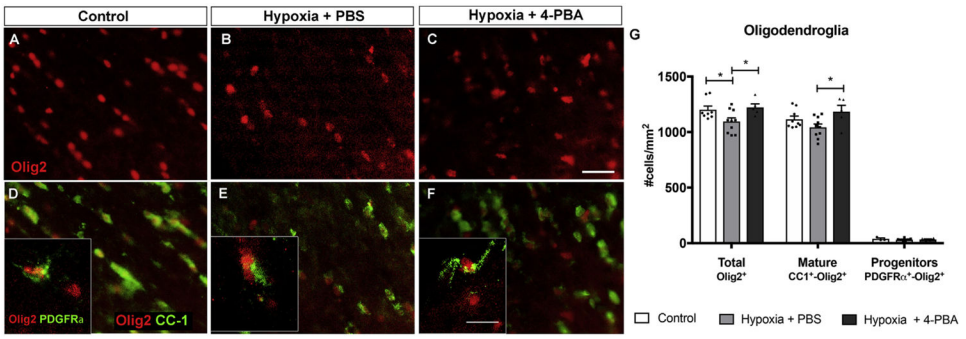

Fig. 4. Hypoxia led to significant loss of Olig2$^+$ cells in the optic nerve, which was completely rescued with treatment with 4-PBA.

A-F: Representative images of total density of oligodendrocytes (Olig2$^+$ cells, **A-C**), mature oligodendrocytes (CC-1$^+$-Olig2$^+$ cells, **D-F)**, and oligodendrocyte progenitors (PDGFRα$^+$-Olig2$^+$ cells, box in **D-F)** in the optic nerve in control (**A, D**), 48 h hypoxia injected with PBS (**B, E**), and 48 h hypoxia treated with 4-PBA (**C, F**). **G:** Bar graph of different oligodendrocyte density in control, 48 h hypoxia injected with PBS, and 48 h hypoxia treated with 4-PBA. Compared with controls, there was significant loss of Olig2$^+$ oligodendrocytes after 48 h hypoxia, and 4-PBA treatment led to significant increase in Olig2$^+$ cells and CC-1$^+$ cells. *P < 0.05, two-way ANOVA with Tukey's multiple comparisons test. Scale bar: 20 μm.

Author Manuscript Author Manuscript Author Manuscript Author Manuscript

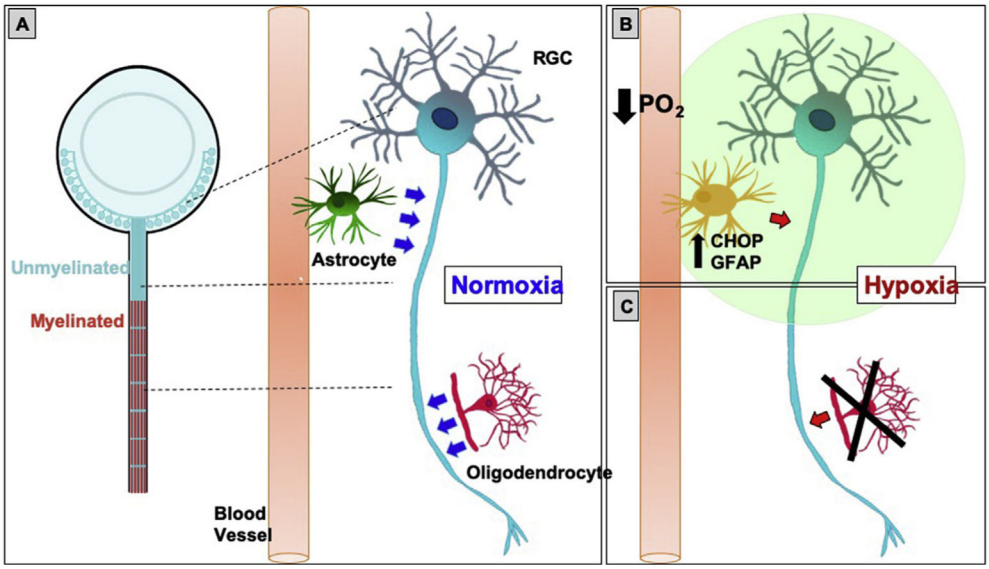

Fig. 5. Proposed model.

A: In normoxia, RGCs are metabolically supported (blue arrows) by astrocytes and oligodendrocytes, the latter only present in the myelinated portion of the optic nerve. **B:** In hypoxia, there is increased CHOP and GFAP co-expression in the unmyelinated portion of the optic nerve, which is consistent with ER stress and reactivity in astrocytes. Combined with loss of oligodendrocytes (**C**), this hypoxic condition creates optic nerve stress, impairing normal homeostasis and metabolic support (red arrows) in the retina and optic nerve. PO_2: partial pressure of oxygen.